EFFECT OF A DAMAGE TO MODAL PARAMETERS OF A WIND TURBINE BLADE

Gunner Chr. Larsen[1], Peter Berring[1], Dmitri Tcherniak[2], Per Hørlyk Nielsen[1], Kim Branner[1]

[1] *DTU Wind Energy, Technical University of Denmark, P.O. Box 49, Roskilde 4000, Denmark*
[2] *Brüel & Kjær SVM, Skodsborgvej 307, Nærum 2850, Denmark*

gula@dtu.dk

ABSTRACT

This study reports structural dynamic characteristics obtained experimentally from an extensive testing campaign on a 34m long wind turbine blade mounted on a test-rig under laboratory conditions. Further, these experimental results have been compared with analog numerical results obtained from a very detailed FE model of the same blade using 3D solid elements. Both an undamaged and a damaged blade are investigated, and it is observed that the natural frequencies of the first few modes of the blade change very little due to a significant artificial damage imposed in trailing edge, whereas the mode shapes - especially if decomposed into the flapwise, edgewise and torsional components - contain information which might be helpful for detecting and localizing wind turbine blade damages.

KEYWORDS : *Dynamic characteristics, FE modeling, OMA, structural damages, wind turbine blade.*

INTRODUCTION

Today, there are no doubts left that Structural Health Monitoring (SHM) becomes a trend in modern civil engineering. Indeed, in many cases it is economically advisable to replace traditional periodic visual checks of the structure with permanent automatic monitoring of its behavior based on sensor readings. This is especially valid for off-shore wind turbines, which in general are expensive and hard to access due to their remote location and associated challenges caused by weather conditions.

One of the challenges a developer of SHM systems will face is the difficulty of testing and verifying the system. Indeed, if a SHM prototype is installed on an operating wind turbine, it may take years before the structure gets damaged, if it ever occurs. The solution to this problem could be simulation environments, where different damages can be modeled, and the *dynamics* of the damaged structure can be simulated. It is then important, that the damage modeling is realistic, in the sense that the dynamic properties of the real damaged structure and its numerical counterpart are the same. This is the topic of the present paper.

The paper describes the full-scale experimental setup, the data processing and the resulting dynamic characteristics for both an undamaged and a damaged blade configuration. The dynamic characteristics of the two blade configurations are subsequently compared with analog numerical results derived from detailed FEM simulations, and conclusions are drawn.

1 EXPERIMENTS

To study and compare the dynamic characteristics of a damaged wind turbine blade and the corresponding undamaged blade, a full-scale 34m blade, manufactured by SSP Technology A/S, was mounted to a test rig under laboratory conditions (cf. Figure 1). The blade was positioned horizontally with the suction side pointing towards the ground.

Figure 1: The 34m blade in the experimental Blade Test Facility at DTU Wind Energy. Left: Suction of blade. Right: Upper (pressure) side of blade. Accelerometers is marked with a red arrow

Several test campaigns were carried out throughout the experiment. The first test was carried out on the undamaged blade. This (reference) test was subsequently followed by tests, where artificial damages were introduced in the trailing edge 18,8m and onwards from the root. In the damaged part of the blade the adhesive between the upper and lower part of the shell was removed to mimic a crack in the trailing edge (cf. Figure 2). The first the damage had a length of 20cm along the blade, and this damage was progressively extended throughout the test campaigns, reaching a length of 120cm in the final test, and thus extending from 18,8m to 20,0m as measured from the blade root. The damaged part of the trailing edge was re-established after tests to enable the blade to be used for other experiments, and the first (reference) tests on the undamaged blade was repeated to investigate whether the re-established trailing edge had affected the dynamic properties of the blade.

Figure 2: The artificial trailing edge damage introduced in the 34m blade

1.1   Instrumentation

Figure 3 sketches the architecture of the measurement system. Twenty triaxial accelerometers B&K Type 4524B were mounted along the blade leading and trailing edges in ten measurement stations located 3.9m; 8m; 11.6m; 14.8m; 17.6m; 20.2m; 22.6m; 24.7m; 26.9m and 28.9m, respectively, from the root).
A substantial effort was made to ensure the position and alignment of the accelerometers in relation to the main axes of the blade, which is a key requirement for a good estimation of the mode shapes.

Since the size and flexibility of the blade prevent the use of conventional tools for measuring lengths and angles, a specially manufactured template was used. Using the template and knowing the geometry of the blade sections, the accelerometers were mounted with sufficiently high precision. Swivel bases B&K Type UA1473 were used to facilitate accelerometer mounting with required orientation.

In order to simplify the measurement setup and reduce the length of the accelerometer cables, a distributed data acquisition system was implemented: every four accelerometers were connected to a 12-ch. data acquisition module B&K Type 3053-B located nearby the accelerometers. The supporting structure was additionally instrumented by 6 triaxial accelerometers (B&K Type 4506). All data acquisition modules were connected to a Cisco Ethernet switch (SG300-10MP), which supports Precise Time Protocol (PTP) and Power over Ethernet (PoE) features. This solves modules' powering and synchronization issues, further reducing the number of cables and the set-up time.
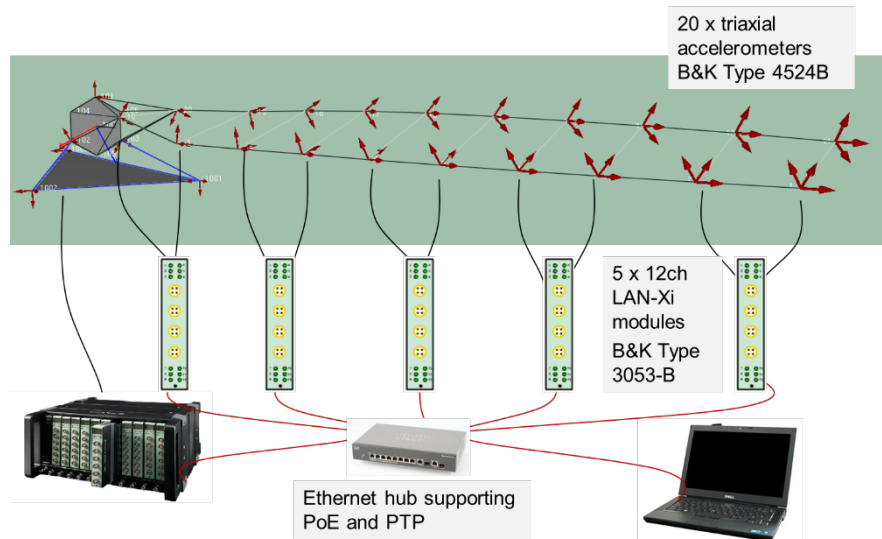

Figure 3: Measurement system architecture. The red arrows show location and orientation of the accelerometers

1.2 Excitation and data acquisition

Since OMA was chosen as dynamics characterization tool, a stochastic excitation needs to be applied. This excitation has to be distributed over the entire structure; be uncorrelated and to have a flat spectrum in the frequency range of interest. In practice, the excitation was performed by several persons hitting the blade at a number of positions using heavy wooden sticks wrapped with foam. An excitation time span of 20 minutes was chosen in order to have a sufficient number of oscillations at the lowest frequency of interest (evaluated to about 1.4Hz). B&K Pulse software was used for data acquisition.

1.3 Data analysis

The experimental data were analyzed using B&K Operational Modal Analysis software Type 7760 (OMA) [1], which, contrary to traditional Modal Analysis (MA), does not require the excitation forces to be recorded, but alternatively *assumes* these to be uncorrelated white noise sources distributed over the entire structure. OMA SSI UPC (Stochastic Subspace Identification, Un-weighted Principal Components) algorithm was utilized.

For each recorded 20 minutes time series, three additional analyses were conducted by splitting the 20 minute time series in three consecutive, partly overlapping, time series, each with a length of 7 minutes. This allowed us to analyze variability of the obtained modal parameters as well as to estimate confidence intervals for experimentally obtained modal parameters. Also, by comparing

the results emerging from each of these three 7 minute time series with the analog results emerging from the full 20 minute time series, the potential influence of recording span lengths was studied.

2 FEM MODELING

The blade dynamics as well as the effect of the damage (trailing edge opening) introduced in the full-scale blade were also investigated numerically using a detailed FE model. The blade was modeled using the commercial finite element pre and post-processor MSC/PATRAN [2]. The model was generated utilizing the DTU Wind Energy's in-house software Blade Modeling Tool (BMT), and MRC/MARC [3] was applied as the solver in all analyses.

2.1 Modeling details

As 20-noded layered continuum elements were used to model the blade structure, a volume representation of the geometry was required. This geometry was generated using BMT together with MSC/PATRAN. 25 cross-sections/aerodynamic profiles were applied in the modeling scheme, which describes the outer geometry of the blade. The curves defining these cross-sections were offset according to the layup definition in order to represent the thickness of the laminates. Finally, the individual cross-sections were connected by spline curves and interpolation surfaces to obtain a volume representation of the blade.

The process described in the previous paragraph was handled automatically by BMT, which in this model utilizes 48 regions/solids to assign the different properties. Variations in thickness between regions results in tapered solids. The model applied in these studies has approximately 40.000 elements. The composite layup was modeled with 15-44 plies though the thickness via BMT, and composite properties were assigned to layered 20-noded continuum elements.

The blade is mounted on a test rig, which is a welded steel construction. This rig was modeled including an estimated flexibility of rig. In these studies the rig is included as a spring/beam system, which is coupled to the blade via a MPC element. Investigations have shown that the flexibility of the rig has only marginal effect on the simulated eigenvalues and eigenvectors of the blade.

The same damage as applied in the experimental test campaign (trailing edge opening) was modeled in the FE model. The adhesive bound was debonded from the lower (pressure side) trailing edge, i.e. the elements were not joined in the interfaces on the area between the adhesive bound and the trailing edge laminate. Contact conditions were, however, not applied in these studies.

The modal analyses were performed by applying the Lanczos method in MSC/MARC. Earlier studies were performed to investigate the effect of including the preloading generated by gravity as a load step before performing the modal analyses. The influence of including gravity turned out to be so limited, that it was decided not to include this in the reported numerical results. An example of a mode shape associated with the damaged blade is shown in Figure 4.
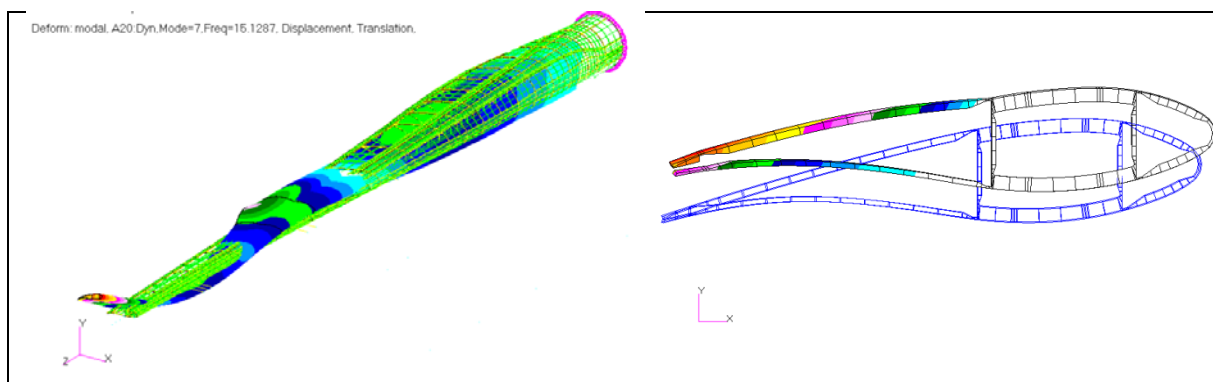

Figure 4: The numerical results of mode 7 of the damaged blade. This mode is primary a combination of flap and edge deflections.

3   RESULTS

The study compares the results from OMA analysis on the full-scale undamaged and damaged blade with the results from respective eigenvalue solutions of the FE models. The lowest 7 natural frequencies (eigen values) together with their associated mode shapes (eigen vectors) are investigated. In addition two higher order experimental modes, without an obvious numerical counterpart but with interesting identification properties, are reported.

As for the experimental analysis, flapwise deflection was defined by $y_c = (y_{LE} + y_{TE})/2$; edge wise deflection was defined by $x_c = (x_{LE} + x_{TE})/2$; and torsion deflection was defined by $\alpha_c = arctan(y_{LE} - y_{TE})$, where $x_{LE}, x_{TE}, y_{LE}, y_{TE}$ are respectively edge- and flapwise displacements of the leading and trailing edges measured at the same radial coordinate of the blade. Note, that the defined torsional deflection differ from a physical rotation, but can be considered as a rotation type parameter amplifying the blade outboard rotations, where the chord lengths are smaller compared to the chord lengths associated with the inner part of the blade.

Figure 5 shows the components of the investigated mode shapes. The left column of the figure displays the FEM results, and the right column shows the corresponding experimental results. Mode shapes referring to the undamaged blade are identified by thick solid lines, whereas mode shapes associated with the damaged blade are plotted as thin dotted lines. Further, red lines refer to flapwise components, blue refers to edge wise components; and green refers to torsion components, respectively. The dashed vertical black lines indicate the boundary of the imposed damage. The experimentally based graphs additionally also show the variability among the experimental mode shapes obtained from the three 7 minute time series and the 20 minute time series, respectively. To ease the comparison between experimental and numerical results, the mode shapes were normalized by defining the tip displacement of the dominating bending modal component as equal to unity.

As for damage detection, two types of "identifier" characteristics can be observed for the *numerical results* corresponding to local and global blade modal type of behavior, respectively. These "identifiers" are predominantly visible in the torsion model component, which is in agreement with the type of damage imposed, where one of the cross sectional cells are opened, and therefore mainly affects the torsion stiffness properties. However, for higher order modes, moderate effects can also be seen in the flap and edge wise modal components. The local modes reflect a local deformation/opening of the blade shell at position of the damage, but with no effect on the blade global deflection pattern. From a practical perspective, such identifiers are not very useful for damage detection, because an unsuitable amount of sensors are required to resolve all possible relevant local modes. This is contrary to damage identifiers based on changes in a blade global mode (e.g. mode 5), where one heuristically can represent the damage as a stiffness "hinge" mainly affecting the blade mode in the regime extending from the damage and to the blade tip. Like for the local modes, information on the damage location is therefore also resulting.

Turning to the *experimental results* little scatter among the four analyzed data sets (i.e 3×7 minute series and the 20 minute series, respectively) is observed for the bending components of the modal shapes. This is contrary to the torsion components, where large variability is observed, especially associated with torsion mode components with very modest amplitudes. This most likely relates to the fact that the torsion signal is derived as the difference between two flapwise signals of comparable size, thus implying relatively high sensitivity to measurement noise/errors. Other explanations could be differences in the damping properties. The main difference between applying 20 minute time series and 7 minute time series is more favorable stabilization diagrams.

Comparing experimentally determined modal shapes with the analog modal shapes resulting from the numerical analysis, a very convincing agreement is found between the *flapwise* and *edge wise* modal components for the investigated first 7 modes. The experimental results do not resolve the *local* damage effects on these modes, but this could not be expected since no accelerometers were positioned at the damage location. As for the *torsion* component, the comparison shows significant differences in shape as well as in magnitude. However, despite the observed shape differences, qualitative similarities are also observed, as global modal effects are seen for the torsion component
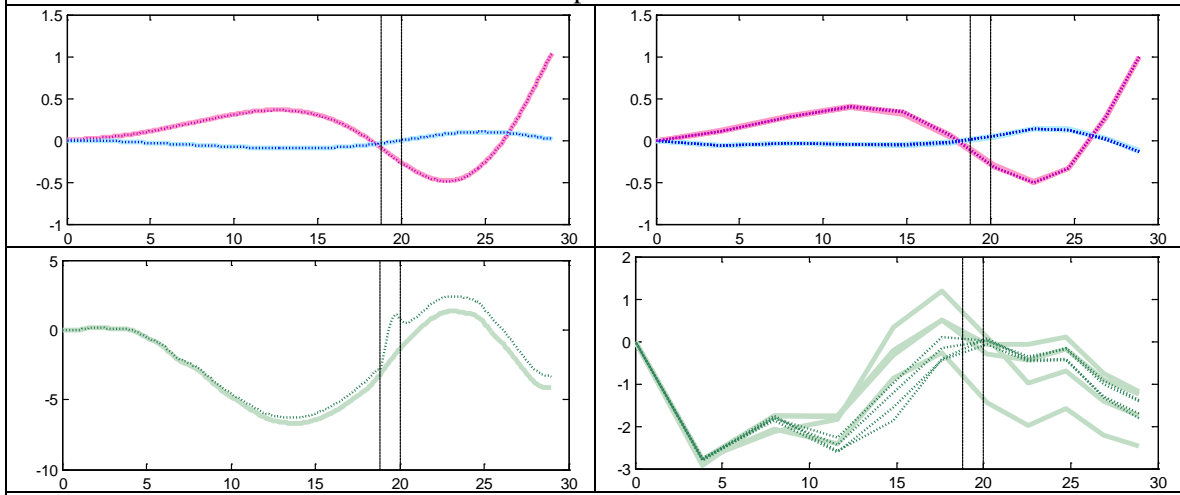
in both experiments and numeric's for mode 3, mode 4 and mode 7, respectively. Consistent with this observation, absolutely no effect of the damage on the global torsion component is observed for mode 6 in the experimental as well as the numerical results.
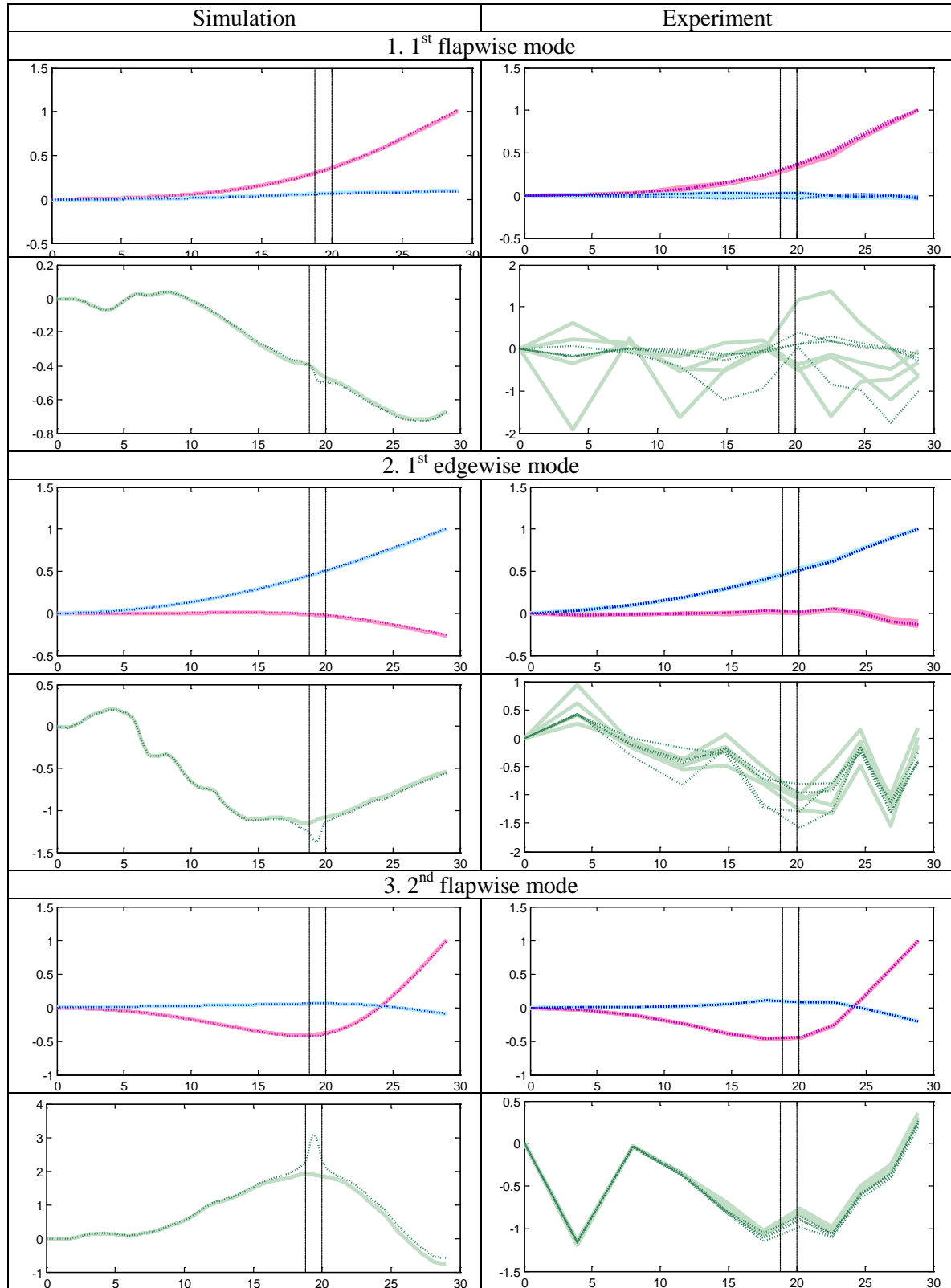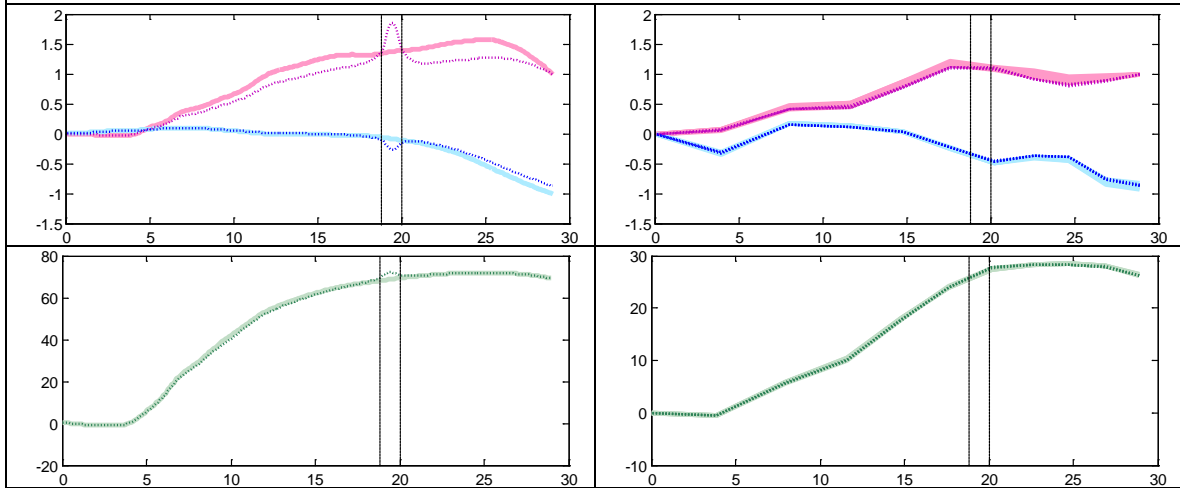
4. 2nd edgewise mode
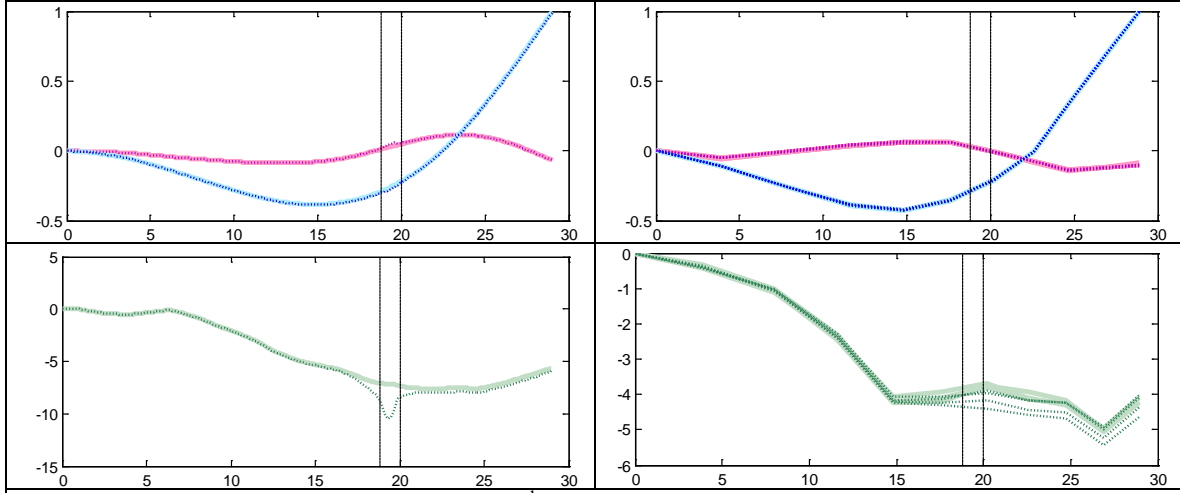
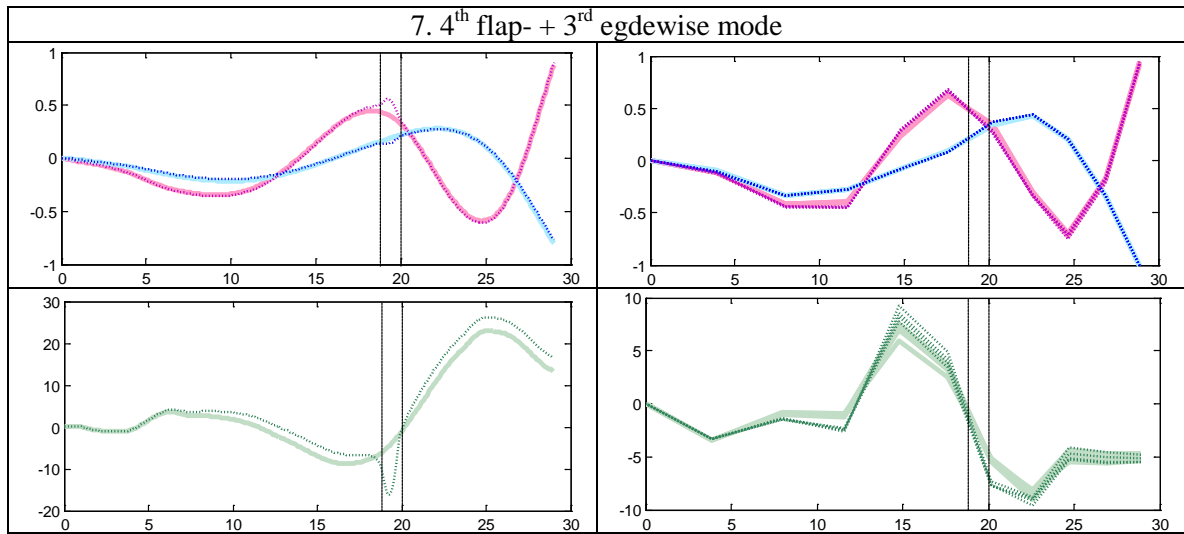5. 3rd flapwise mode

6. 1st torsional mode

Figure 5: Blade mode shapes. Left column: numerical results; right column: experimental results.

Additionally two higher order modes are identified by OMA, which cannot directly be paired with analog modes from the numerical analysis. These modes show relative high sensitivity to the damage, and they are therefore included and shown in Figure 6.
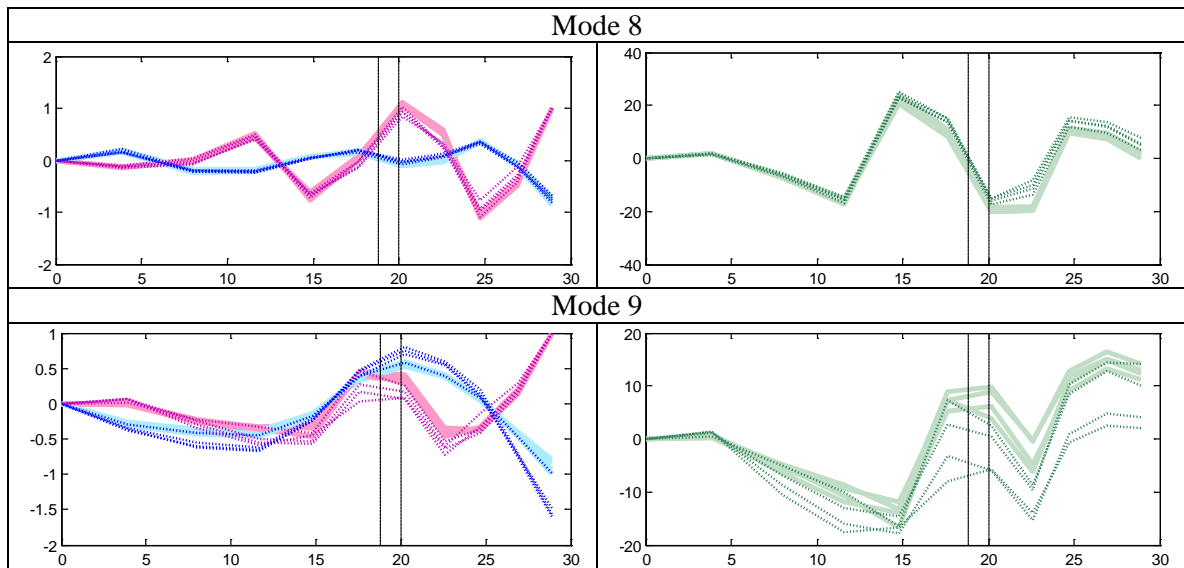

Figure 6: Higher order experimental mode shapes with high sensitivity to the imposed damage

Finally, the results for the corresponding natural frequencies are shown in Table 1 for the two blade configurations and including both the experiment and the numerical analysis.

Table 1: Simulated and measured natural frequencies for the damaged and the undamaged blade

Mode	Name	Damaged blade		Undamaged blade	
		OMA [Hz]	FEM [Hz]	OMA [Hz]	FEM [Hz]
Mode 1	1st flap	1.36	1.37	1.36	1.38
Mode 2	1st edge	1.86	1.81	1.86	1.80
Mode 3	2nd flap	4.21	4.20	4.21	4.22
Mode 4	2nd edge	7.12	7.09	7.12	7.10
Mode 5	3rd flap	9.17	9.39	9.19	9.41
Mode 6	1st torsion	12.4	11.8	12.4	11.9
Mode 7	4th flap + 3rd edge	15.0	15.1	15.0	15.2

As seen good agreement is observed between predicted and measured natural frequencies for both the undamaged and the damaged blade. It is furthermore seen, that the natural frequencies display no sensitivity to the investigated damage for all practical purposes.

CONCLUSION

A very convincing agreement between measured and simulated results has been demonstrated for the natural frequencies as well as for the bending components of the mode shapes. However, significant differences in shape and/or magnitude are observed for the torsion components of the mode shapes, especially when associated with torsion mode components with very modest amplitudes.

It was also observed that the natural frequencies of the investigated modes of the blade change very little due to the imposed trailing edge damage, with changes being significantly below the uncertainties of OMA. However, the mode shapes, when decomposed into the flapwise, edgewise and torsional components contain information, which might be helpful for detecting and localizing damages in the trailing edge of the blade.

ACKNOWLEDGEMENTS

REFERENCES

[1] Zhang L, Brincker R, and Andersen P. 2005. An Overview of Operational Modal Analysis: Major Development and Issues, Proc. of 1st Int. Operational Modal Analysis Conference (IOMAC-2005).

[2] MSC/PATRAN. MSC Software Corporation: Patran [cited May 2014]. Available from: http://www.mscsoftware.com/product/patran.

[3] MSC/MARC. MSC Software Corporation: Marc [cited May 2014]. Available from: http://www.mscsoftware.com/product/marc.